

Measurement of the Quark Mixing Parameter $\cos 2\phi_1$ Using Time-Dependent Dalitz Analysis of $\bar{B}^0 \rightarrow D[K_S^0 \pi^+ \pi^-] h^0$

P. Krokovny,⁵ K. Abe,⁵ K. Abe,³⁶ I. Adachi,⁵ H. Aihara,³⁸ D. Anipko,¹ K. Arinstein,¹ Y. Asano,⁴¹ V. Aulchenko,¹ T. Aushev,⁸ S. Bahinipati,³ A. M. Bakich,³³ V. Balagura,⁸ E. Barberio,¹⁵ A. Bay,¹³ U. Bitenc,⁹ I. Bizjak,⁹ A. Bondar,¹ A. Bozek,²¹ M. Bračko,^{5,14,9} T. E. Browder,⁴ Y. Chao,²⁰ A. Chen,¹⁸ W. T. Chen,¹⁸ Y. Choi,³² A. Chuvikov,²⁸ S. Cole,³³ J. Dalseno,¹⁵ M. Danilov,⁸ M. Dash,⁴² S. Eidelman,¹ D. Epifanov,¹ S. Fratina,⁹ N. Gabyshev,¹ A. Garmash,²⁸ T. Gershon,⁵ A. Go,¹⁸ A. Gorišek,⁹ H. Ha,¹¹ K. Hayasaka,¹⁶ H. Hayashii,¹⁷ M. Hazumi,⁵ D. Heffernan,²⁵ T. Higuchi,⁵ L. Hinz,¹³ T. Hokuue,¹⁶ Y. Hoshi,³⁶ S. Hou,¹⁸ W.-S. Hou,²⁰ Y. B. Hsiung,²⁰ T. Iijima,¹⁶ K. Ikado,¹⁶ A. Imoto,¹⁷ K. Inami,¹⁶ A. Ishikawa,³⁸ H. Ishino,³⁹ R. Itoh,⁵ M. Iwasaki,³⁸ Y. Iwasaki,⁵ J. H. Kang,⁴³ N. Katayama,⁵ H. Kawai,² T. Kawasaki,²³ H. Kichimi,⁵ H. J. Kim,¹² S. M. Kim,³² K. Kinoshita,³ S. Korpar,^{14,9} P. Križan,^{44,9} R. Kulasiri,³ R. Kumar,²⁶ C. C. Kuo,¹⁸ A. Kuzmin,¹ Y.-J. Kwon,⁴³ J. Lee,³⁰ T. Lesiak,²¹ J. Li,²⁹ S.-W. Lin,²⁰ G. Majumder,³⁴ T. Matsumoto,⁴⁰ S. McOnie,³³ W. Mitaroff,⁶ K. Miyabayashi,¹⁷ Y. Miyazaki,¹⁶ T. Mori,³⁹ I. Nakamura,⁵ M. Nakao,⁵ S. Nishida,⁵ T. Nozaki,⁵ S. Ogawa,³⁵ T. Ohshima,¹⁶ T. Okabe,¹⁶ S. Okuno,¹⁰ H. Ozaki,⁵ P. Pakhlov,⁸ C. W. Park,³² H. Park,¹² L. S. Peak,³³ R. Pestotnik,⁹ L. E. Piilonen,⁴² A. Poluektov,¹ M. Rozanska,²¹ Y. Sakai,⁵ T. R. Sarangi,⁵ N. Sato,¹⁶ N. Satoyama,³¹ T. Schietinger,¹³ O. Schneider,¹³ K. Senyo,¹⁶ H. Shibuya,³⁵ B. Shwartz,¹ J. B. Singh,²⁶ A. Sokolov,⁷ A. Somov,³ N. Soni,²⁶ R. Stamen,⁵ M. Starič,⁹ H. Stoeck,³³ K. Sumisawa,²⁵ O. Tajima,⁵ F. Takasaki,⁵ K. Tamai,⁵ M. Tanaka,⁵ Y. Teramoto,²⁴ X. C. Tian,²⁷ K. Trabelsi,⁴ T. Tsuboyama,⁵ T. Tsukamoto,⁵ S. Uehara,⁵ K. Ueno,²⁰ S. Uno,⁵ P. Urquijo,¹⁵ Y. Ushiroda,⁵ G. Varner,⁴ K. E. Varvell,³³ S. Villa,¹³ C. C. Wang,²⁰ C. H. Wang,¹⁹ Y. Watanabe,³⁹ E. Won,¹¹ B. D. Yabsley,³³ A. Yamaguchi,³⁷ Y. Yamashita,²² M. Yamauchi,⁵ J. Ying,²⁷ L. M. Zhang,²⁹ Z. P. Zhang,²⁹ and V. Zhilich¹

(Belle Collaboration)

¹*Budker Institute of Nuclear Physics, Novosibirsk*

²*Chiba University, Chiba*

³*University of Cincinnati, Cincinnati, Ohio 45221*

⁴*University of Hawaii, Honolulu, Hawaii 96822*

⁵*High Energy Accelerator Research Organization (KEK), Tsukuba*

⁶*Institute of High Energy Physics, Vienna*

⁷*Institute of High Energy Physics, Protvino*

⁸*Institute for Theoretical and Experimental Physics, Moscow*

⁹*J. Stefan Institute, Ljubljana*

¹⁰*Kanagawa University, Yokohama*

¹¹*Korea University, Seoul*

¹²*Kyungpook National University, Taegu*

¹³*Swiss Federal Institute of Technology of Lausanne, EPFL, Lausanne*

¹⁴*University of Maribor, Maribor*

¹⁵*University of Melbourne, Victoria*

¹⁶*Nagoya University, Nagoya*

¹⁷*Nara Women's University, Nara*

¹⁸*National Central University, Chung-li*

¹⁹*National United University, Miao Li*

²⁰*Department of Physics, National Taiwan University, Taipei*

²¹*H. Niewodniczanski Institute of Nuclear Physics, Krakow*

²²*Nippon Dental University, Niigata*

²³*Niigata University, Niigata*

²⁴*Osaka City University, Osaka*

²⁵*Osaka University, Osaka*

²⁶*Panjab University, Chandigarh*

²⁷*Peking University, Beijing*

²⁸*Princeton University, Princeton, New Jersey 08544*

²⁹*University of Science and Technology of China, Hefei*

³⁰*Seoul National University, Seoul*

³¹*Shinshu University, Nagano*

³²*Sungkyunkwan University, Suwon*

³³University of Sydney, Sydney NSW³⁴Tata Institute of Fundamental Research, Bombay³⁵Toho University, Funabashi³⁶Tohoku Gakuin University, Tagajo³⁷Tohoku University, Sendai³⁸Department of Physics, University of Tokyo, Tokyo³⁹Tokyo Institute of Technology, Tokyo⁴⁰Tokyo Metropolitan University, Tokyo⁴¹University of Tsukuba, Tsukuba⁴²Virginia Polytechnic Institute and State University, Blacksburg, Virginia 24061⁴³Yonsei University, Seoul⁴⁴University of Ljubljana, Ljubljana

(Received 8 May 2006; published 24 August 2006)

We present a measurement of the angle ϕ_1 of the Cabibbo-Kobayashi-Maskawa unitarity triangle using a time-dependent Dalitz analysis of $D \rightarrow K_S^0 \pi^+ \pi^-$ decays produced in neutral B meson decay to a neutral D meson and a light meson ($\bar{B}^0 \rightarrow D^{(*)} h^0$). The method allows a direct extraction of $2\phi_1$ and, therefore, helps to resolve the ambiguity between $2\phi_1$ and $\pi - 2\phi_1$ in the measurement of $\sin 2\phi_1$. We obtain $\sin 2\phi_1 = 0.78 \pm 0.44 \pm 0.22$ and $\cos 2\phi_1 = 1.87^{+0.40+0.22}_{-0.53-0.32}$. The sign of $\cos 2\phi_1$ is determined to be positive at 98.3% C.L.

DOI: 10.1103/PhysRevLett.97.081801

PACS numbers: 12.15.Hh, 11.30.Er, 13.25.Hw

Precise determination of the Cabibbo-Kobayashi-Maskawa (CKM) matrix elements [1] is important to check the consistency of the standard model (SM) and search for new physics. The value of $\sin 2\phi_1$, where ϕ_1 is one of the angles of the unitarity triangle, is now measured with high precision: $\sin 2\phi_1 = 0.725 \pm 0.037$ [2,3]. This leads to four solutions in ϕ_1 : 23° , 67° , $(23 + 180)^\circ$, and $(67 + 180)^\circ$. Resolution of this ambiguity has been attempted using time-dependent angular analysis in the $B^0 \rightarrow J/\psi K^{*0}(K_S^0 \pi^0)$ decay. This technique provides a measurement of $\cos 2\phi_1$ and therefore helps to distinguish between the solutions at 23° and 67° [4,5].

A new technique based on the analysis of $\bar{B}^0 \rightarrow D[K_S^0 \pi^+ \pi^-] h^0$ has been recently suggested [6]. Here we use h^0 to denote light neutral mesons, π^0 , η , and ω . The neutral D meson is reconstructed in the $K_S^0 \pi^+ \pi^-$ decay mode; its resonant substructure has been measured [7,8].

Consider a neutral B meson that is known to be a \bar{B}^0 at time t_{tag} . At another time, t_{sig} , its state is given by

$$|\bar{B}^0(\Delta t)\rangle = e^{-|\Delta t|/2\tau_{B^0}} \times \left[|\bar{B}^0\rangle \cos(\Delta m \Delta t/2) - i \frac{D}{q} |B^0\rangle \sin(\Delta m \Delta t/2) \right], \quad (1)$$

where $\Delta t = t_{\text{sig}} - t_{\text{tag}}$, τ_{B^0} is the average lifetime of the B^0 meson, Δm , p , and q are parameters of B^0 - \bar{B}^0 mixing. Here we have assumed CPT invariance and neglected terms related to the lifetime difference of neutral B mesons. In the SM, $|q/p| = 1$ to a good approximation, and, in the usual phase convention, $\arg(p/q) = 2\phi_1$.

The $B \rightarrow Dh^0$ decay amplitude is dominated by the CKM favored $b \rightarrow c\bar{u}d$ diagram as shown in Fig. 1, with roughly a 2% contribution from the CKM suppressed $b \rightarrow u\bar{c}d$ diagram. Ignoring the latter, a neutral D meson produced in a \bar{B}^0 decay is a D^0 , while that produced in a B^0 decay is a \bar{D}^0 . The D meson state produced at time Δt is then given by $|D^0\rangle \cos(\Delta m \Delta t/2) - ie^{2i\phi_1} \xi_{h^0} (-1)^l |\bar{D}^0\rangle \times \sin(\Delta m \Delta t/2)$, where we use ξ_{h^0} to denote the CP eigenvalue of h^0 , and l gives the orbital angular momentum in the Dh^0 system. In the case of $\bar{B}^0 \rightarrow D^* h^0$, an additional factor arises due to the CP properties of the particle emitted in the D^* decay (either $D^* \rightarrow D\pi^0$ or $D^* \rightarrow D\gamma$) [9].

We follow Ref. [8] and describe the amplitude for a $\bar{D}^0 \rightarrow K_S^0 \pi^+ \pi^-$ decay as $f(m_+^2, m_-^2)$, where m_+^2 and m_-^2 are the squares of the two-body invariant masses of the $K_S^0 \pi^+$ and $K_S^0 \pi^-$ combinations. Assuming no CP violation in the neutral D meson system, the amplitude for a D^0 decay is then given by $f(m_-^2, m_+^2)$. The time-dependent Dalitz plot density is defined by

$$P(m_+^2, m_-^2, \Delta t, q_B) = \frac{e^{-|\Delta t|/\tau_{B^0}}}{8\tau_{B^0}} \frac{F(m_+^2, m_-^2)}{2N} (1 + q_B \times \{\mathcal{A}(m_-^2, m_+^2) \cos(\Delta m \Delta t) + \mathcal{S}(m_-^2, m_+^2) \sin(\Delta m \Delta t)\}),$$

$$\mathcal{A} = (|f(m_-^2, m_+^2)|^2 - |f(m_+^2, m_-^2)|^2)/F(m_+^2, m_-^2), \quad \mathcal{S} = \frac{-2\xi_{h^0} (-1)^l \text{Im}\{f(m_-^2, m_+^2) f^*(m_+^2, m_-^2) e^{2i\phi_1}\}}{F(m_+^2, m_-^2)}, \quad (2)$$

$$F = |f(m_-^2, m_+^2)|^2 + |f(m_+^2, m_-^2)|^2, \quad N = \int |f(m_-^2, m_+^2)|^2 dm_+^2 dm_-^2,$$

where the b -flavor charge is $q_B = +1$ (-1) when the tagging B meson is a B^0 (\bar{B}^0). Thus the phase $2\phi_1$ can be extracted from a time-dependent Dalitz plot fit to B^0 and \bar{B}^0 data if $f(m_+^2, m_-^2)$ is known. Note that this formulation assumes that there is no direct CP violation in the B decay amplitudes.

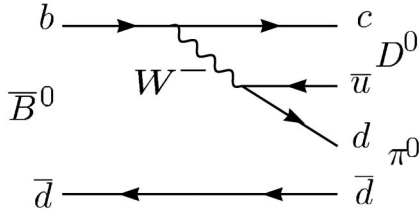


FIG. 1. Diagram for the dominant color-suppressed amplitude for $\bar{B}^0 \rightarrow D\pi^0$.

This analysis is based on $386 \times 10^6 B\bar{B}$ events collected with the Belle detector at the asymmetric energy e^+e^- collider [10]. The Belle detector has been described elsewhere [11]. We reconstruct the decays $\bar{B}^0 \rightarrow Dh^0$ for $h^0 = \pi^0, \eta$ and ω and $\bar{B}^0 \rightarrow D^*h^0$ for $h^0 = \pi^0$ and η .

Charged tracks are selected based on the number of hits and impact parameter relative to the interaction point (IP). To reduce combinatorial background, a transverse momentum of at least 0.1 GeV/c is required of each track. All charged tracks that are not positively identified as electrons are treated as pions.

Neutral kaons are reconstructed via the decay $K_S^0 \rightarrow \pi^+\pi^-$. The $\pi\pi$ invariant mass is required to be within 9 MeV/c² ($\sim 3\sigma$) of the K^0 mass, and the displacement of the $\pi^+\pi^-$ vertex from the IP in the transverse (r - ϕ) plane is required to have a magnitude between 0.2 cm and 20 cm and a direction that agrees within 0.2 radians with the combined momentum of the two pions.

Photon candidates are selected from calorimeter showers not associated with charged tracks. An energy deposition of at least 50 MeV and a photonlike shape are required for each candidate. A pair of photons with an invariant mass within 12 MeV/c² (2.5σ) of the π^0 mass is considered as a π^0 candidate.

We reconstruct neutral D mesons in the $K_S^0\pi^+\pi^-$ decay channel and require the invariant mass to be within 15 MeV/c² (2.5σ) of the nominal D^0 mass. D^{*0} candidates are reconstructed in the $D^0\pi^0$ decay channel. The mass difference between D^{*0} and D^0 candidates is required to be within 3 MeV/c² of the expected value (3σ). ω candidates are reconstructed in the $\pi^+\pi^-\pi^0$ decay channel. Their invariant mass is required to be within 20 MeV/c² (2.5Γ) of the ω mass. We define the angle θ_ω between the normal to the ω decay plane and opposite of the B direction in the rest frame of ω and require $|\cos\theta_\omega| > 0.3$. We reconstruct η candidates in the $\gamma\gamma$ and $\pi^+\pi^-\pi^0$ final states and require the invariant mass to be within 10 and 30 MeV/c² (2.5σ) of the η mass, respectively. The photon energy threshold for the prompt π^0 and η candidates coming from B decays is increased to 200 MeV in order to reduce combinatorial background. We remove η candidates if either of the daughter photons can be combined with any other photon with $E_\gamma > 100$ MeV to form a π^0 candidate.

We combine either D and $h^0 = \{\pi^0, \omega, \eta\}$ or D^* and $h^0 = \{\pi^0, \eta\}$ to form B mesons. Signal candidates are identified by their energy difference in the center-of-mass (c.m.) system of the $Y(4S)$, $\Delta E = (\sum_i E_i) - E_{\text{beam}}$, and the beam-energy constrained mass, $M_{\text{bc}} = \sqrt{E_{\text{beam}}^2 - (\sum_i \vec{p}_i)^2}$, where E_{beam} is the beam energy and \vec{p}_i and E_i are the momenta and energies of the decay products of the B meson in the c.m. frame. The masses of π^0, η , and $D^{(*)}$ candidates are constrained to their nominal values to improve ΔE resolution. We select events with $M_{\text{bc}} > 5.2$ GeV/c² and $|\Delta E| < 0.3$ GeV, and define the signal region to be 5.272 GeV/c² $< M_{\text{bc}} < 5.287$ GeV/c², -0.1 GeV $< \Delta E < 0.06$ GeV ($\pi^0, \eta \rightarrow \gamma\gamma$), or $|\Delta E| < 0.03$ GeV ($\omega, \eta \rightarrow \pi^+\pi^-\pi^0$). In cases with more than one candidate in an event, the one with D and h^0 masses closest to the nominal values is chosen.

To suppress the large combinatorial background dominated by the two-jetlike $e^+e^- \rightarrow q\bar{q}$ continuum process, variables that characterize the event topology are used. We require $|\cos\theta_{\text{thr}}| < 0.80$, where θ_{thr} is the angle between the thrust axis of the B candidate and that of the rest of the event. This requirement eliminates 77% of the continuum background and retains 78% of the signal. We also construct a Fisher discriminant, \mathcal{F} , which is based on the production angle of the B candidate, the angle of the B candidate thrust axis with respect to the beam axis, and nine parameters that characterize the momentum flow in the event relative to the B candidate thrust axis in the c.m. frame [12]. We impose a requirement on \mathcal{F} that rejects 67% of the remaining continuum background and retains 83% of the signal.

Signal yields and background levels are determined by fitting distributions in ΔE for candidates in the M_{bc} signal region. For each mode, the ΔE distribution is fitted with an asymmetric Gaussian for signal and a linear function for background. The signal shape is fixed, based on MC simulation. The region $\Delta E < -0.1$ GeV is excluded from the fit to avoid contributions from other B decays. The results from our fits to the data are shown in Fig. 2 and Table I. We study the systematic error of the fit by varying the shapes for signal and background and changing the fit range. The difference in the signal yields does not exceed 5%. We also confirm that there is no feed across between channels and other peaking background by using generic $B\bar{B}$ MC calculations.

The signal B decay vertex is reconstructed using the D trajectory and the IP constraint. The tagging B vertex is obtained with well-reconstructed tracks not assigned to the signal B candidate and the IP constraint [13]. The time difference between signal and tagging B candidates is calculated using $\Delta t = \Delta z / \gamma\beta c$ and $\Delta z = z_{CP} - z_{\text{tag}}$. The proper-time interval resolution function $R_{\text{sig}}(\Delta t)$ is formed by convolving four components: the event-by-event detector resolutions for z_{CP} and z_{tag} , the shift in the z_{tag} vertex position due to secondary tracks originating

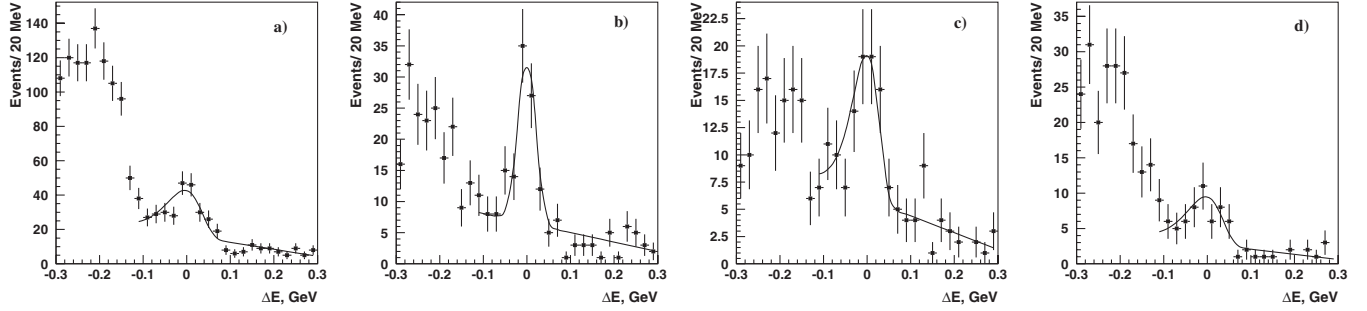


FIG. 2. ΔE distributions for the \bar{B}^0 decays to (a) $D\pi^0$, (b) $D\omega$, (c) $D\eta$, and (d) $D^*\pi^0$, $D^*\eta$. Points with error bars represent the data and curves show the results of the fit.

from charmed particle decays, and the kinematic approximation that B mesons are at rest in the c.m. frame [13]. A small component of broad outliers in the Δz distribution, caused by misreconstruction, is represented by a Gaussian function. Charged leptons, pions, kaons, and Λ baryons that are not associated with a reconstructed $\bar{B}^0 \rightarrow D[K_S^0 \pi^+ \pi^-] h^0$ decay are used to identify the b flavor of the accompanying B meson. The tagging algorithm is described in detail elsewhere [14].

We perform an unbinned time-dependent Dalitz plot fit. The negative logarithm of the unbinned likelihood function is minimized:

$$-2 \log L = -2 \sum_{i=1}^n \log\{(1 - f_{\text{bg}})P_{\text{sig}} + f_{\text{bg}}P_{\text{bg}}\}, \quad (3)$$

where n is the number of events. The function $P_{\text{sig}}(m_+^2, m_-^2, \Delta t)$ is the time-dependent Dalitz plot density for the signal events, which is calculated according to Eq. (2) and incorporates reconstruction efficiency, flavor-tagging efficiency, wrong tagging probability, and Δt resolution. The function P_{bg} is the probability density function (PDF) for the background. Both P_{sig} and P_{bg} are normalized by $\int P_{\text{sig,bg}}(m_+^2, m_-^2, \Delta t) dm_+^2 dm_-^2 d\Delta t = 1$. The event-by-event background fraction $f_{\text{bg}}(\Delta E, M_{\text{bc}})$ is based on signal and background levels found by fitting ΔE as described above, the ΔE shape used in the fit, and an M_{bc} shape that is the sum of a Gaussian signal and an empirical background function with kinematic threshold and shape parameters determined from off-resonance data.

TABLE I. Number of events in the signal region (N_{tot}), detection efficiency, number of signal events from the ΔE fit (N_{sig}), and signal purity for the $B \rightarrow D^{(*)} h^0$ final states.

Process	N_{tot}	Efficiency (%)	N_{sig}	Purity
$D\pi^0$	265	8.7	157 ± 24	59%
$D\omega$	88	4.1	67 ± 10	76%
$D\eta$	101	3.9	58 ± 13	57%
$D^*\pi^0, D^*\eta$	67		43 ± 12	64%
Sum	521		325 ± 31	62%

We describe the background by the sum of four components: B decays containing (a) real D mesons and (b) combinatorial D mesons, and $q\bar{q}$ events containing (c) real D mesons and (d) combinatorial D mesons. The Dalitz plot is described by the function $f(m_+^2, m_-^2)$ for (a) and (c). For (b) and (d) we use an empirical background function which includes enhancements near the edges of the Dalitz plot as well as an incoherently added $K^*(892)$ contribution [8]. The shape of this function is obtained from an analysis of events in the D mass sideband. The Δt distribution for the B decay backgrounds is described by an exponential convolved with the detector resolution. For the $q\bar{q}$ background, a triple Gaussian form is used, which is obtained from events with $|\cos\theta_{\text{thr}}| > 0.8$. The use of this sideband region has been validated using MC calculations. We use the experimental data and generic MC calculations to fix the fractions of background components. Figure 3 shows the Dalitz plot distributions for candidates in signal and M_{bc} sideband region, integrated over the entire Δt range and B^0 and \bar{B}^0 combined. We can see clear differences in these distributions.

The procedure for the Δt fit is tested by extracting τ_{B^+} using $B^+ \rightarrow \bar{D}^0[K_S^0 \pi^+ \pi^-] \pi^+$ decay. We obtain $\tau_{B^+} = 1.678 \pm 0.043$ ps (statistical error only), consistent with the PDG [2] value 1.638 ± 0.011 ps.

We perform a fit by fixing τ_{B^0} and Δm at the PDG values with a fixed background shape and using $\sin 2\phi_1$, $\cos 2\phi_1$ as fitting parameters. The results are given in Table II for each of the three final states separately and for the simultaneous fit over all modes.

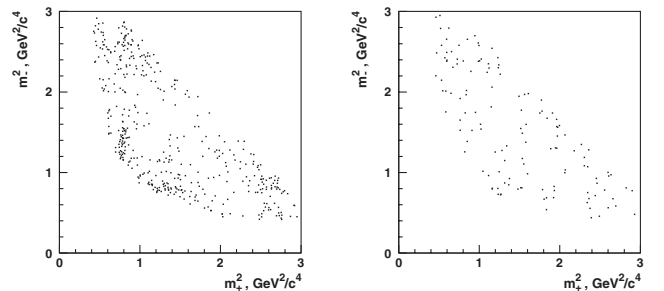


FIG. 3. Dalitz plot distribution for the Dh^0 candidates from B signal region (left) and M_{bc} sideband.

TABLE II. Fit results for the data. Errors are statistical only.

Final state	$\sin 2\phi_1$	$\cos 2\phi_1$
$D\pi^0, D\eta[\gamma\gamma]$	$0.80^{+0.54}_{-0.60}$	$2.07^{+0.78}_{-0.91}$
$D\omega, D\eta[3\pi]$	0.43 ± 0.90	$1.53^{+0.67}_{-0.93}$
$D^*\pi^0, D^*\eta$	1.07 ± 1.14	$3.46^{+1.80}_{-2.01}$
Simultaneous fit	0.78 ± 0.44	$1.87^{+0.40}_{-0.53}$

We check goodness-of-fit using one-dimensional projections to $K_S^0\pi^\pm$ and $\pi^+\pi^-$ invariant masses and δt and find no pathological behavior. To illustrate, the raw CP asymmetry distribution for $D^{(*)}h^0$ candidates with an additional constraint $|M_{\pi^+\pi^-} - 0.77| < 0.15 \text{ GeV}/c^2$, to select events consistent with $D \rightarrow K_S^0\rho$, is displayed in Fig. 4. For D^*h^0 candidates we take into account the opposite CP asymmetry. In this case the system behaves approximately as a CP eigenstate, with an asymmetry proportional to $-\sin 2\phi_1$.

Uncertainty of the $D \rightarrow K_S^0\pi^+\pi^-$ decay model is one of the main sources of systematic error for our analysis. We repeat the fit using two additional decay models from CLEO [7] and similar Belle analysis [15]. The difference between these models and our primary model [8] is in describing of wide resonances in $\pi^+\pi^-$ and $K_S^0\pi$, non-resonant part and doubly Cabibbo suppressed channels. The CLEO [7] does not include wide resonances $\sigma(600)$ and $f_0(1370)$, and the doubly Cabibbo suppressed channel $D^0 \rightarrow K^{*+}(1430)\pi^-$. Another Belle model [15] has an additional contributions from $K^*(1410)^\pm pi^\mp$ and $K_S^0\rho^0(1450)$. The difference in fitted values for $\sin 2\phi_1$ and $\cos 2\phi_1$ between the nominal model [8] and others is found not to exceed 0.1, and we assign this value as a model uncertainty.

We vary the background descriptions to estimate the systematic uncertainty due to the background parametrization. We use only a combinatorial and only a signal D PDF for the Dalitz plot distribution. For the time dependence,

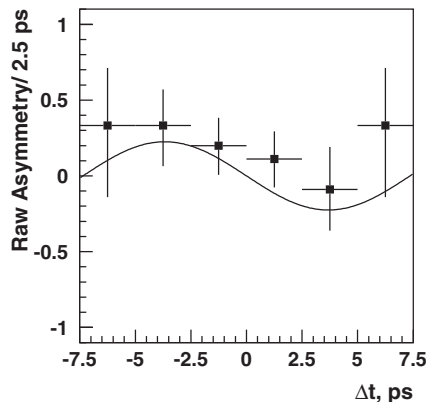


FIG. 4. Raw asymmetry distribution for the $D^{(*)}[K_S^0\rho^0]h^0$ candidates. The smooth curve is the result of the fit to the full Dalitz plot.

we consider cases with only a $q\bar{q}$ component or only a $B\bar{B}$ component. The differences do not exceed 0.2 and we take this value as a systematic error.

Other contributions to the systematic error are found to be small: vertexing and flavor tagging (0.02), neglecting suppressed amplitudes (0.01), and signal yield determination (0.02).

The measurement of $\sin 2\phi_1 = 0.78 \pm 0.44 \pm 0.22$ is consistent with the high statistics measurement in the $J/\psi K^0$ channel [2]. The result of $\cos 2\phi_1 = 1.87^{+0.40+0.22}_{-0.53-0.32}$ allows one to distinguish between two solutions in ϕ_1 : 23° and 67° . We define the confidence level at which the 67° solution (negative value of $\cos 2\phi_1$) can be excluded as $\text{C.L.}(x) = f_+(x)/[f_+(x) + f_-(x)]$, where $f_+(x)$ [$f_-(x)$] is the likelihood to obtain the fit result $\cos 2\phi_1 = x$ when true $\cos 2\phi_1$ value of 0.689 (-0.689). To evaluate f_+ and f_- we use sample of 2500 pseudoexperiments with the same size as data for both hypotheses. We fit these distributions with a sum of two Gaussians. We calculate C.L. for $x = 1.87, 1.55, \text{ and } 2.09$ to take into account systematic uncertainties of $^{+0.22}_{-0.32}$ in our $\cos 2\phi_1$ measurement. As a final result we use the smallest value $\text{C.L.}(1.55) = 98.5 \pm 0.2\%$, excluding the 67° solution at 98.3% C.L.

In summary, we have presented a new method to measure the unitarity triangle angle ϕ_1 using a time-dependent amplitude analysis of the $D \rightarrow K_S^0\pi^+\pi^-$ decay produced in the processes $\bar{B}^0 \rightarrow D^{(*)}h^0$. We find $\sin 2\phi_1 = 0.78 \pm 0.44 \pm 0.22$ and $\cos 2\phi_1 = 1.87^{+0.40+0.22}_{-0.53-0.32}$. The sign of $\cos 2\phi_1$ is determined to be positive at 98.3% C.L., favoring the $\phi_1 = 23^\circ$ solution.

We thank the KEKB group for excellent operation of the accelerator, the KEK cryogenics group for efficient solenoid operations, and the KEK computer group and the NII for valuable computing and Super-SINET network support. We acknowledge support from MEXT and JSPS (Japan); ARC and DEST (Australia); NSFC and KIP of CAS (Contracts No. 10575109 and No. IHEP-U-503, China); DST (India); the BK21 program of MOEHRD, and the CHEP SRC and BR (Grant No. R01-2005-000-10089-0) programs of KOSEF (Korea); KBN (Contract No. 2P03B 01324, Poland); MIST (Russia); ARRS (Slovenia); SNSF (Switzerland); NSC and MOE (Taiwan); and DOE (USA).

- [1] M. Kobayashi and T. Maskawa, Prog. Theor. Phys. **49**, 652 (1973); N. Cabibbo, Phys. Rev. Lett. **10**, 531 (1963).
- [2] S. Eidelman *et al.*, Phys. Lett. B **592**, 1 (2004), <http://pdg.lbl.gov>.
- [3] B. Aubert *et al.* (BABAR Collaboration), Phys. Rev. Lett. **94**, 161803 (2005); K. Abe *et al.* (Belle Collaboration), Phys. Rev. D **71**, 072003 (2005).
- [4] B. Aubert *et al.* (BABAR Collaboration), Phys. Rev. D **71**, 032005 (2005).
- [5] R. Itoh and Y. Onuki *et al.* (Belle Collaboration), Phys. Rev. Lett. **95**, 091601 (2005).

- [6] A. Bondar, T. Gershon, and P. Krokovny, Phys. Lett. B **624**, 1 (2005).
- [7] H. Muramatsu *et al.* (CLEO Collaboration), Phys. Rev. Lett. **89**, 251802 (2002); **90**, 059901(E) (2003).
- [8] A. Poluektov *et al.* (Belle Collaboration), Phys. Rev. D **70**, 072003 (2004).
- [9] A. Bondar and T. Gershon, Phys. Rev. D **70**, 091503(R) (2004).
- [10] S. Kurokawa and E. Kikutani, Nucl. Instrum. Methods Phys. Res., Sect. A **499**, 1 (2003).
- [11] A. Abashian *et al.*, Nucl. Instrum. Methods Phys. Res., Sect. A **479**, 117 (2002).
- [12] A. Garmash *et al.* (Belle Collaboration), Phys. Rev. D **65**, 092005 (2002).
- [13] H. Tajima *et al.*, Nucl. Instrum. Methods Phys. Res., Sect. A **533**, 370 (2004).
- [14] H. Kakuno *et al.*, Nucl. Instrum. Methods Phys. Res., Sect. A **533**, 516 (2004).
- [15] A. Poluektov *et al.* (Belle Collaboration), Phys. Rev. D **73**, 112009 (2006).